Supporting Information

In order to relate measured EFM data to physical quantities, Eqn. (3) is derived:
Claim:

$$\tan(\Delta\phi) \cong -\frac{Q}{k}\frac{\partial F}{\partial z} \tag{S1}$$

where ϕ, Q, and k, are the phase, quality factor, and spring constant, respectively.

Derivation, from Sarid p. 27, eq. 2.40, 2.41[1]:

$$\tan(\phi) = \frac{\frac{\omega}{Q\omega_0}}{\frac{{\omega'_0}^2 - \omega^2}{\omega_0^2}} = \frac{\omega\omega_0}{Q\left({\omega'_0}^2 - \omega^2\right)} \tag{S2}$$

For tip operated near resonance: $\omega \cong \omega_0$

$$\tan(\phi) = \frac{\omega_0^2}{Q\left({\omega'_0}^2 - \omega_0^2\right)} = \frac{1}{Q\left(\left(\frac{\omega'_0}{\omega_0}\right)^2 - 1\right)} \tag{S3}$$

For small gradients we have:

$$-\frac{1}{2k}\frac{\partial F}{\partial z} \cong 1 - \frac{\omega'_0}{\omega_0} \tag{S4}$$

$$\frac{\omega'_0}{\omega_0} \cong 1 + \frac{1}{2k}\frac{\partial F}{\partial z} \rightarrow \left(\frac{\omega'_0}{\omega_0}\right)^2 \cong 1 + \frac{1}{k}\frac{\partial F}{\partial z} + \frac{1}{4k^2}\left(\frac{\partial F}{\partial z}\right)^2 \tag{S5}$$

and since $\frac{\partial F}{\partial z}$ is small,

$$\left(\frac{\omega'_0}{\omega_0}\right)^2 \cong 1 + \frac{1}{k}\frac{\partial F}{\partial z} \tag{S6}$$

Therefore:

$$\tan(\phi) \cong \frac{1}{Q\left(1 + \frac{1}{k}\frac{\partial F}{\partial z} - 1\right)} = \frac{1}{Q\left(\frac{1}{k}\frac{\partial F}{\partial z}\right)} \tag{S7}$$

$$\cot(\phi) \cong \frac{Q}{k}\frac{\partial F}{\partial z} \tag{S8}$$

Near resonance $\phi = \frac{\pi}{2} + \Delta\phi \rightarrow \cot(\phi) = -\tan(\Delta\phi)$, thus:

$$\tan(\Delta\phi) \cong -\frac{Q}{k}\frac{\partial F}{\partial z} \tag{S9}$$

Discussion of EFM Model. As mentioned in the text, the sphere-to-plane capacitor does not completely describe the physical system of the tip-to-surface. This becomes apparent when examining Eq 6 and solving for its roots by using the Quadratic Equation. The nature of the roots of a quadratic equation is revealed by examining the discriminant, $\sqrt{b^2 - 4ac}$.

In our case,

$$\sqrt{\left(\frac{3R^2 q_s}{2z}\right)^2 - 4 \cdot (-2\pi\varepsilon_0 R^2)\left(-\frac{q_s^2}{2\pi\varepsilon_0}\right)}$$

$$\sqrt{\frac{9R^4 q_s{}^2}{4z^2} - 4 \cdot R^2 q_s^2}$$

$$\frac{Rq_s}{2z}\sqrt{9R^2 - 16z^2}$$

Evidently, the parabolas formed by plotting $\tan(\Delta\phi)$ against V_{tip} have real roots only if

$$9R^2 \geq 16z^2$$

$$\frac{z}{R} \leq \frac{3}{4}$$

which is impossible by the conditions of using the approximation in the first place. This conclusion implies that the parabolas in Figure 4d should never cross the x-axis and the contrast inversion observed in Figure 4b should not occur. These contradictory results indicate that the sphere-to-plane capacitor model does not describe the tip-to-sample system with high accuracy. Nevertheless, the model is useful as a first order approximation to determine the sign of the injected charge carriers. Since the data reported in Figure 4b were taken at $V_{tip} = 0$, they are free of inaccuracies that result from the deficiencies of this model.

Figure S1 displays typical effects of measuring SWCNT-TFTs in air *verses* measuring the devices in vacuum following extended desorption. With extended desorption, the hysteresis reduces by ~3 V, the forward-sweep p-type threshold voltage shifts by -3 V, and the presence of an electron channel becomes apparent. Similar changes are observed in SWCNT-TFTs with both high-k dielectric materials (Al_2O_3 and HfO_2) used in this study. The lack of an electron channel when measured in air suggests Fermi level pinning due to electron transfer from the

SWCNTs into the surrounding water solvated oxygen redox couple.[2] As reported in Table 1, the

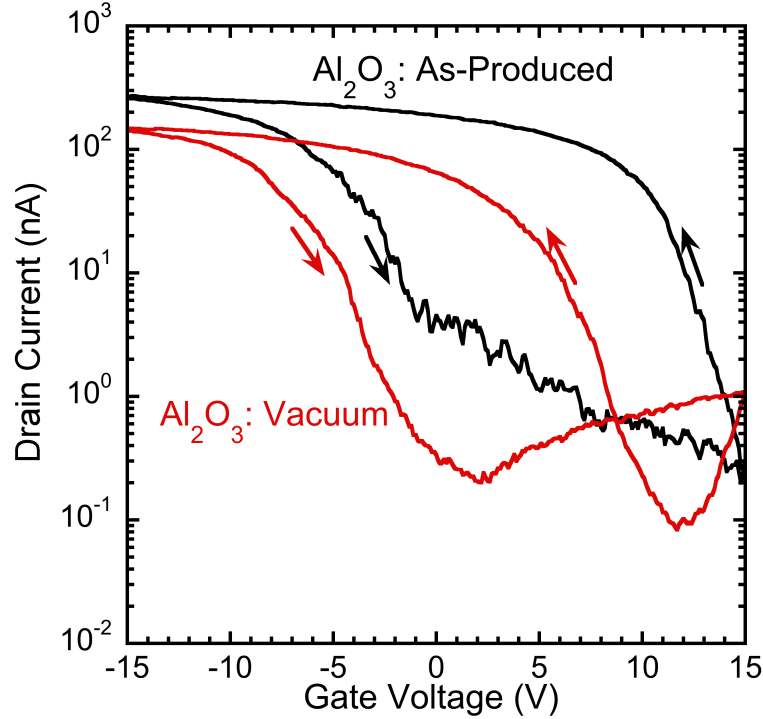p-type hysteresis is **positive** for both dielectric layers.

Figure S1. Gate transfer characteristics for the same device (Al_2O_3 on SiO_2) measured in air immediately after fabrication (black-line) and measured in vacuum ($<1\times10^{-5}$ Torr) following heating at 325 K for at least 12 hours (red-line).

Figure S2 displays the capacitance-voltage (CV) characteristics for metal-oxide-semiconductors

(MOS) measured on as-grown high-κ dielectrics and high-κ dielectrics annealed prior to

metallization. In these measurements, the Si substrate serves as the semiconductor (no SWCNTs

are present), which is accumulated, depleted, or inverted by applying a bias between it and a top

metal electrode. The CV scan begins with a 5 s soak at -5 V, proceeds through depletion to hole

accumulation at high Si gate voltage, then returns. For the as-grown high-k dielectrics, no

inversion is observed in the MOS CV measurements at low gate voltage, and the inflection near

7.5 V is characteristic of interface trapped charge, Q_{it}, at the SiO_2:Si interface. The hysteresis in

these samples is +0.7 V and +1.9 V for Al_2O_3 and HfO_2, respectively and reduces to +0.3 V and

+0.4 V for MOS capacitors annealed prior to metallization. Additionally, the annealed samples show inversion at low Si gate voltage and the inflection associated with Q_{it} is no longer present, suggesting that Fermi level pinning by the interface trapped charges effects the inversion layer formation (measured at 10 kHz) in the as-grown MOS structures. The hysteresis observed near inversion is common in MOS devices and results from insufficient time to form the inversion layer after sweeping through depletion. Regardless of its origin, the direction of the hysteresis near accumulation is **_negative_**. This is **_opposite_** to the hysteresis we observed in the SWCNT-TFT devices. This confirms that neither charge injection at the metal electrodes, charge inject at the Si back gate, nor mobile ions within the gate dielectric layers are the primary source of the hysteresis observed in SWCNT-TFTs with high-k dielectric layers analyzed in this study.
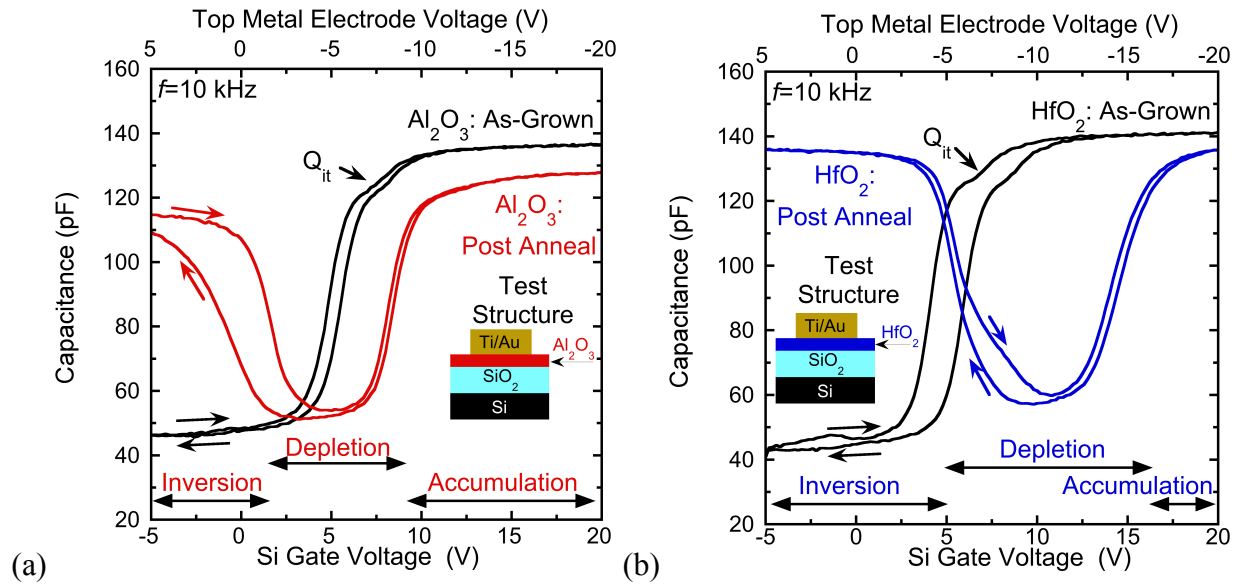

Figure S2. Capacitance-voltage curves for (a) Al_2O_3 and (b) HfO_2 dielectrics on SiO_2:Si wafers with test structure configures as shown as insets in both parts of the figure. In both parts, the black curve is the as-grown ALD material, while the colored line corresponds with the capacitance-voltage characteristics for the films following a 1 minute 1000° C anneal in N_2. The bottom x-axis labels indicate the Si voltage with respect to a grounded top metal electrode consistent with SWCNT-TFT gate voltage sweeps. The top x-axis label indicates the top metal electrode voltage in reference to a grounded Si substrate, and is the typical configuration for metal-oxide-semiconductor capacitance-voltage measurements.

1. Sarid, D. *Scanning Force Microscopy*; Oxford University Press: New York, 1991.
2. Aguirre, C. M.; Levesque, P. L.; Paillet, M.; Lapointe, F.; St-Antoine, B. C.; Desjardins, P.; Martel, R. The Role of the Oxygen/Water Redox Couple in Suppressing Electron Conduction in Field-Effect Transistors. *Adv Mater* **2009**, *21*, 3087–3091.